Published in final edited form as:
Eur J Nucl Med Mol Imaging. 2010 August ; 37(9): 1710–1721. doi:10.1007/s00259-010-1441-1.

SIMULTANEOUS DUAL-RADIONUCLIDE MYOCARDIAL PERFUSION IMAGING WITH A SOLID-STATE DEDICATED CARDIAC CAMERA

S. Ben-Haim[1], **K. Kacperski**[1], **S. Hain**[1], **D. Van Gramberg**[1], **B.F. Hutton**[1], **W.A. Waddington**[1], **T. Sharir**[2], **N. Roth**[3], **D.S. Berman**[4], and **P.J. Ell**[1]

[1]Institute of Nuclear Medicine, University college London Hospitals, NHS Trust, London, United Kingdom

[2]Procardia-Maccabi Healthcare services, Tel-Aviv, Israel

[3]Spectrum-Dynamics, Caesarea, Israel

[4]Cedars Sinai Medical center, Los Angeles, California

Abstract

We compared simultaneous dual-radionuclide stress and rest myocardial perfusion imaging (MPI) with a novel solid-state cardiac camera and a conventional SPECT camera with separate stress and rest acquisitions.

Methods—24 consecutive patients (64.5 ± 11.8 years, 16 men) were injected with 74 MBq of ^{201}Tl (rest) and 250 MBq ^{99m}Tc-MIBI (stress). Conventional MPI acquisition times for stress and rest were 21 min and 16 min, respectively. A simultaneous dual-radionuclide (DR) 15 minute list mode gated acquisition was performed on D-SPECT (Spectrum-dynamics, Caesarea, Israel). The DR D-SPECT data were processed using a spillover and scatter correction method. We compared DR D-SPECT images with conventional SPECT images by visual analysis employing the 17-segment model and a 5-point scale (0=normal, 4=absent) to calculate the summed stress and rest scores (SSS and SRS, respectively) and the % visual perfusion defect (TPD) at stress and rest, by dividing the stress and rest scores, respectively, by 68 and multiplying by 100. TPD <5% was considered normal. Image quality was assessed on a 4-point scale (1=poor, 4=very good) and gut activity was assessed on a 4-point scale (0=none, 3=high).

Results—Conventional MPI was abnormal at stress in 17 patients and at rest in 9 patients. In the 17 abnormal stress studies DR D-SPECT MPI was abnormal in 113 vs. 93 abnormal segments by conventional MPI. In the nine abnormal rest studies DR D-SPECT was abnormal in 45 vs. 48 segments abnormal by conventional MPI. SSS, SRS, TPD stress and TPD rest on conventional SPECT and DR D-SPECT highly correlated (r=0.9790, 0.9694, 0.9784, 0.9710, respectively; p<0.0001 for all). In addition, 6 patients had significantly larger perfusion defects on DR D-SPECT stress images, including five of 11 patients who were imaged earlier on D-SPECT than conventional SPECT.

Conclusion—D-SPECT enables fast and high quality simultaneous DR MPI in a single imaging session with comparable diagnostic performance and image quality to conventional SPECT. Modifications of the injected doses and of the imaging protocol with DR D-SPECT may enable

Correspondence: Simona Ben-Haim, MD, DSc, Honorary Professor and Consultant Physician, Institute of Nuclear Medicine, University College London Hospital NHS Trust, 235 Euston Road T5, London NW1 2BU, UK, Telephone: +44 (0)20 7380 9424, Fax: +44 (0)20 7436 0603, Simona.ben-haim@uclh.nhs.uk.

Europe PMC Funders Author Manuscripts

shortening of imaging time, reducing radiation exposure and shortening significantly patient stay in the department.

Keywords

Myocardial perfusion imaging; simultaneous dual-radionuclide acquisition; early imaging; cardiac camera; solid state detectors

Europe PMC Funders Author Manuscripts

INTRODUCTION

Myocardial perfusion imaging SPECT (MPI) has a well established role for diagnosis, prognosis and risk stratification in the management of patients with known or suspected coronary artery disease. Currently MPI is performed in two separate imaging sessions, at rest and after stress, and the 2 sets of images are compared to assess for perfusion abnormalities. Whether ^{201}Tl or ^{99m}Tc labelled radionuclides are used this is a lengthy procedure, requiring about 40min imaging time for the two sessions and usually waiting time of about 3 hours in between.

Recently the D-SPECT cardiac scanner (Spectrum-Dynamics, Caesarea, Israel) has been introduced, based on a novel detector design and acquisition geometry, as well as reconstruction algorithm (1-4). Briefly, nine pixelated solid-state detector columns with cadmium-zinc telluride (CZT) crystals and wide-angle tungsten collimators, combined with a novel image reconstruction algorithm, provide region-of-interest centric scanning localized to the heart. Compared to a standard gamma camera, this system provides up to 8 fold increase in count rate, while achieving increase in spatial resolution compared to conventional SPECT with filtered back projection (1, 3-5). The use of CZT crystals enables improved energy resolution: at 140keV 5.5% compared to 10% energy resolution of a conventional camera. This may therefore potentially enable simultaneous acquisition of several radionuclides, which would be of most interest for MPI, offering a single imaging session with exact image registration between the two image sets at rest and post stress.

The superior energy resolution permits the discrimination of photons of different energy which can result not only in reduced scatter but also in the case of Tungsten collimators an ability to discriminate Tungsten X rays from the ^{201}Tl photopeak. An appealing extension is to simultaneously image ^{99m}Tc and ^{201}Tl in a combined rest/stress protocol. We therefore evaluated the accuracy and image quality of simultaneous dual radionuclide (DR) MPI employing D-SPECT with ^{201}Tl rest and ^{99m}Tc sestamibi stress imaging in comparison with sequential dual radionuclide MPI using a conventional SPECT.

MATERIAL AND METHODS

Patient population

Twenty –seven patients with history of ischemic heart disease were prospectively recruited from the routine referral base at University College London Hospital (Institute of Nuclear Medicine) between November 2007 and July 2008. Three patients were excluded due to technical reasons, so the study population includes 24 patients. The study was approved by the local ethics committee. All patients signed an informed consent.

Adenosine stress protocol

Patients were instructed to avoid caffeine-containing products for at least 12 hours and dipyridamole and xanthine preparations for 24 hours before the test. Adenosine (140 μg/kg/

Europe PMC Funders Author Manuscripts

min) was infused over 6 minutes ^{99m}Tc sestamibi was injected at 4 minutes after start of the infusion. All patients performed low-level bicycle exercise during adenosine infusion.

Conventional SPECT acquisition and processing protocol

Images were obtained with a dual-head camera (Infinia, GE Healthcare, Haifa, Israel) equipped with low-energy high-resolution collimator (for ^{99m}Tc sestamibi imaging) or low-energy general purpose collimator (for ^{201}Tl imaging). 80 MBq of ^{201}Tl were injected at rest and imaging started as soon as possible after the injection. Images were acquired with 30 projections per detector over 180° orbit, for 40 seconds/projection (imaging time 21 minutes). Images were reconstructed with filtered back projection, and a Hann filter with 0.75 cut-off was applied.

For the stress images 250 MBq of ^{99m}Tc sestamibi were injected during adenosine infusion. Images were acquired with 30 projections over 180° orbit, for 30 sec/projection, 45-160 minutes (average 65.6±30.35 min) after the injection (imaging time 16 minutes). Images were reconstructed with filtered back projection, and a Hann filter with 0.75 cut-off was applied. No attenuation or scatter correction was applied.

D-SPECT acquisition and processing protocol

A 15 min list mode simultaneous dual radionuclide (rest/stress) gated acquisition (120 projection/detector, 7.5 sec/projection) was performed. The D-SPECT images (DR D-SPECT) were acquired 75.7±45.8 minutes after the adenosine infusion. In 13 patients the conventional SPECT stress images were followed by DR D-SPECT, whereas in 11 patients the DR D-SPECT acquisition was performed before conventional SPECT stress acquisition. In these 11 patients DR D-SPECT was performed 35.4±28.8 minutes after stress injection (range: 15-91), compared to 76.5±38.5, range: 45-160 minutes after stress injection for conventional SPECT. In the remaining 13 patients images were acquired 107.2±34.25 minutes post stress injection (range: 66-184), compared to 68.2±35.84, range 20-160 minutes after stress injection for conventional SPECT.

The DR D-SPECT images were acquired at 177.4 ± 51.8 minutes post rest injection of ^{201}Tl (range: 15-75 minutes) compared to conventional SPECT rest images which were acquired 38.5 ±13.8 min after ^{201}Tl injection (range: 15-75 minutes).

Data were acquired in a semi-reclining position with the left arm resting on top of the camera. A 30-second pre-scan was performed prior to the acquisition to identify the location of the heart and to set the angle limits of scanning for each detector, enabling region of interest (ROI)-centric scanning.

The data were processed using a spillover and scatter correction (SC) method, specifically designed for D-SPECT. Briefly, the availability of list mode data permits the retrospective selection of several energy windows corresponding to the photopeaks for ^{99m}Tc (140keV) and ^{201}Tl (70keV and 167 keV) and selected ‘scatter’ windows positioned below each of the photopeaks (6). A representative energy spectrum is illustrated in Figure 1 which demonstrates the windows selected. Note that the measurements in the various windows can be considered to consist of several components a) photopeak counts from one of the radionuclides b) scatter counts deriving from one or both radionuclides c) counts that are detected with reduced energy due to various effects in the solid state detector. Estimates of the spatial distribution of these latter two sources of photons were determined by measurement of point sources and used to establish a set of six equations that describe the relative contributions in each of the six energy windows. These were used to determine scatter-free estimates for the photopeak ^{99m}Tc and ^{201}Tl counts (6).

Transaxial images were generated by a proprietary reconstruction algorithm (Broadview™, Spectrum-Dynamics, Caesarea, Israel), based on the ordered subsets expectation maximization method (OSEM) (3, 7). Transaxial images were reoriented into short-axis and vertical and horizontal long-axis slices using quantitative perfusion SPECT software (QPS, Cedars-Sinai Medical Center, Los Angeles, California).

Visual analysis of perfusion images

Conventional SPECT and D-SPECT images were visually assessed in consensus by two experienced Nuclear Medicine physicians (SBH, SH) on separate occasions, blinded to the scores given to the other imaging. Images were semi-quantitatively scored using a 17-segment model of the left ventricle and a 5-point scale (0=normal, 1=mild, 2=moderate, 3=severe reduction of tracer uptake and 4=absent tracer uptake). The global summed stress score (SSS) and summed rest score (SRS) were calculated by adding the scores of the 17 segments in stress and rest images, respectively. The % visual perfusion abnormality at stress and rest was then calculated by dividing the stress and rest scores, respectively, by 68 (17 × 4, maximum score) and multiplying by 100. Perfusion abnormality <5% was considered normal (5). An abnormal segment was defined as score > 1.

In addition, image quality was assessed for the two imaging methods on a 4-point scale (1=poor, 4=very good). Gut activity was assessed on a 4-point scale (0=none, 1=low, 2=medium, 3=high gut activity).

Invasive coronary angiography

Invasive coronary angiography results within 3 months of MPI with no intervening coronary event, procedure or change in symptoms were available in five patients. Angiographic results were obtained from the clinical angiographic report. A stenosis with ≥50% lumen diameter narrowing was considered significant CAD.

Statistical Analysis

Continuous variables are presented as mean ± SD. Correlation between SSS, SRS and % visual perfusion abnormality by DR D-SPECT and conventional SPECT were evaluated by linear regression. %TPD differences of ≥5% were deemed significant. Agreement between two methods was assessed by Bland-Altman analysis. A p value <0.05 was considered significant.

RESULTS

Patient characteristics

The clinical characteristics of the patient population are depicted in Table 1. There were 24 patients (16 men, 66%) with a mean age of 64.5 ± 11.8 years and a mean BMI of 25.6±2.64. Twenty one patients (88%) had previously known CAD and seven (29%) had previous infarcts.

Correlation of perfusion images

Rest images—There were 9 abnormal conventional SPECT rest studies; all of these were also abnormal on DR D-SPECT. Two additional conventional SPECT rest studies with reduced uptake in the inferior wall; neither of these patients had history or ECG evidence of prior MI. DR D-SPECT rest images were normal, suggesting that the conventional SPECT defects were due to attenuation artifacts..

A total of 408 segments were analyzed at rest. Forty-eight segments (12%) were abnormal on conventional SPECT ^{201}Tl rest images and 45 (11%) were abnormal on DR D-SPECT.

There was excellent linear correlation between SRS and % rest TPD by conventional SPECT versus SRS and % rest TPD obtained from the simultaneous DR acquisition on D-SPECT (r= 0.9694, r= 0.9710, p<0.0001) (Figures 2, 3). On Bland-Altman analysis there was very good agreement between the two imaging methods with a small shift for both SRS and %TPD rest (mean difference 0.79, 95% confidence interval −2.459-0.428 for SRS; mean difference 1.16, 95% confidence interval −3.54-0.627 for %TPD rest).

Stress images—There were 17 abnormal conventional SPECT stress studies; all of these were also abnormal on D-SPECT. However, 3 DR D-SPECT stress studies were technically suboptimal due to gut activity adjacent to the inferior myocardial wall interfering with the interpretation of the studies and these were excluded from further analysis. These patients were imaged on DR-DSPECT earlier than conventional SPECT (DR D-SPECT at 15, 20 and 90 minutes post stress injection compared to 52, 55 and 160, minutes post injection respectively on conventional SPECT).

A total of 357 myocardial segments were assessed. There were 93 abnormal segments (26%) on conventional SPECT stress images and 113 abnormal segments (32%) on the D-SPECT stress images obtained from simultaneous DR acquisition.

There was excellent linear correlation between SSS and % stress TPD by conventional SPECT versus SSS and % stress TPD obtained from the simultaneous DR acquisition on DSPECT (r= 0.9790, r= 0.9784, p<0.0001) (Figure 4). On Bland-Altman analysis there was very good agreement between the two imaging methods with a shift for both SSS and %TPD stress (mean difference −2.0, 95% confidence interval −2.392-1.991 for SSS; mean difference −3.0, 95% confidence interval −3.42-3.076 for % TPD stress).

Discrepant studies—The discrepant studies are summarized in Tables 2 and 3. Of the 21 stress studies analyzed, in 6 cases perfusion defects were significantly larger on DR D-SPECT stress images than on conventional SPECT (%TPD difference ≥5%) (Table 2, Figure 5). In five of these patients DR D-SPECT images were acquired before conventional SPECT (18 – 47 minutes post stress injection for DR D-SPECT compared to 45 – 100 minutes post stress injection for conventional SPECT) and in one patient DR D-SPECT acquisition was performed after conventional SPECT. The larger perfusion defects were seen in the antero-apical region (5 patients), septum (4 cases), lateral wall (2 cases) and in one case in the inferior wall. None of the patients showed a larger stress defect on conventional SPECT compared to the D-SPECT.

Significant differences in rest % TPD (≥5%) were noted in 3 patients (Table 3). One patient showed significantly smaller perfusion defects and more inducible ischemia on DR-DSPECT compared to conventional SPECT (patient 17, Table 3, DR difference of 12%) and in two other patients the differences were less prominent (patients 11 and 19, TPD differences 6% and 5%, respectively, table 3). None of the patients showed a larger rest defect on conventional SPECT compared to DR D-SPECT.

Image quality—Image quality was good or very good in 22/24 conventional SPECT stress studies and in all 24 conventional rest studies. Simultaneous DR D-SPECT images were graded as good or very good in 21/24 for the stress component and in all 24 for the rest component of the study.

On conventional SPECT stress ^{99m}Tc MIBI studies there was low or absent gut activity in 13 cases, moderate in 2 and high in 9 cases. On the conventional SPECT rest ^{201}Tl studies gut activity was low or absent in 14, moderate in 4 and high in 6 cases.

On the stress component of the simultaneous DR D-SPECT studies there was high gut activity in 16 cases (3 of these were excluded from analysis), moderate activity in 2 cases and low or absent activity in 6. In the rest component of the study there was low or absent gut activity in 22 cases and high activity in two.

Correlation with coronary angiography—Tables 4 and 5 summarize the findings in coronary angiography, conventional SPECT and simultaneous DR D-SPECT of the 5 patients who underwent coronary angiography.

A good correlation was observed between the MPI findings by both nuclear imaging techniques compared with the angiographic data. All five patients had evidence of CAD by angiography with stenoses in the LCX and OM1 branch in 4 cases, in the LAD and D1 in 3 cases and in the RCA in 3 cases. In three cases there was good correlation between the extent and severity of the perfusion abnormalities on DR D-SPECT and conventional SPECT MPI and both were concordant with the angiographic findings. Whereas in two cases, patients 19 and 25, there were larger stress perfusion defects and more inducible ischemia on the simultaneous DR D-SPECT study compared to conventional SPECT (Table 4).

A patient with more severe and extensive stress induced defects on DR D-SPECT compared to conventional SPECT is illustrated in Figure 5.

DISCUSSION

Sequential dual isotope imaging with rest ^{201}Tl/stress ^{99m}Tc sestamibi has been recommended in the past so that the stress ^{99m}Tc images are not interfering with the ^{201}Tl images (8). Recently Berman et al. have demonstrated a rapid sequential stress ^{201}Tl/ rest ^{99m}Tc imaging protocol of less than 30 minutes in total with D-SPECT (9). However, since the solid state D-SPECT camera shows improved energy resolution for CZT compared to that obtained with NaI with good energy separation for multiple radionuclides (4), simultaneous imaging with multiple radionuclides is possible with D-SPECT as has been demonstrated in the current manuscript. Correction is needed to correct for spillover from the higher energy radionuclide to the lower energy radionuclide, as well as spillover resulting from broad photopeak tails that are present in the pixelated CZT detector (6). The significantly improved sensitivity of D-SPECT compared to conventional gamma cameras enables the use of lower injected activity to reduce the spillover fraction. Preliminary data suggest that simultaneous dual radionuclide imaging is feasible with D-SPECT (10).

A single imaging procedure acquiring simultaneously stress and rest data is highly desirable for myocardial perfusion imaging, enabling exact registration of both data sets. This may enable improved detection of small changes in regional perfusion and is likely to allow easier detection of attenuation artifacts. In addition, imaging time can be significantly reduced, increasing patient throughput and shortening patient stay in the clinic. Only few studies with simultaneous DR imaging were previously performed on conventional gamma cameras (11-13). However, the lower energy ^{201}Tl window data were substantially contaminated by the higher energy and higher activity of ^{99m}Tc. In addition the lead X-rays originating from the ^{99m}Tc activity can also confound the results and therefore this protocol was eventually abandoned. Recently, Steele at al. have assessed a prototype triple-detector

multi-pinhole SPECT system for ^{201}Tl stress/^{99m}Tc rest myocardial perfusion imaging, showing promising results (14).

The current study is the first clinical study of simultaneous DR myocardial perfusion imaging on a solid state dedicated cardiac camera. The solid state detectors along with the spillover and scatter correction reconstruction enable a single 15 minute list mode acquisition with D-SPECT, compared to two separate stress and rest acquisitions for 16 and 21 minutes respectively, about two hours apart. All normal and abnormal studies were correctly characterized on DR D-SPECT. There is high correlation between stress and rest perfusion scores by DR D-SPECT and conventional SPECT (0.98 and 0.97, respectively) with good agreement and small shifts on Bland-Altman analysis. The results of the present study demonstrate comparable diagnostic performance and image quality of both imaging modalities, while shortening imaging time and enabling to shorten significantly patient stay in the department with D-SPECT.

Of interest, in six of the 21 stress studies analyzed (29%) perfusion defects on the DR D-SPECT stress images were larger than on the corresponding conventional SPECT images, including five of 11 cases with early post stress DR D-SPECT imaging compared to conventional SPECT (45%) and one case imaged after conventional SPECT. In one case (Figure 5), with coronary angiography available for comparison, the early DR D-SPECT stress images with larger perfusion abnormalities correlated better with the angiographic findings. Similar findings have been previously reported with ^{99m}Tc-tetrofosmin (12, 15). Schulz et al. (16) found the relative washout fraction per hour of tetrofosmin was 8.3% ±9.9% in areas with a stress-induced defect. Ito et al. compared dual-isotope acquisitions of both ^{201}Tl and ^{99m}Tc-tetrofosmin at stress and rest in 27 patients. ^{99m}Tc-tetrofosmin images were performed twice, 10 minutes and 70 minutes after stress injection and the defects at 10 minutes post stress were significantly larger than the defects at 70 minutes post stress. Furthermore, a significantly higher washout rate of tetrofosmin from normal segments was demonstrated compared to ischemic segments between the early and late imaging and therefore perfusion defects in ischemic segments appeared smaller on the delayed scan. In some cases with ^{201}Tl redistribution the authors have also observed “redistribution” of ^{99m}Tc-tetrofosmin between the early and delayed stress acquisition. Therefore the authors recommend acquiring ^{99m}Tc-tetrofosmin stress images within 10-35 minutes post stress (12). Giorgetti et al. reported on 120 patients who underwent ^{99m}Tc-tetrofosmin myocardial perfusion imaging at 15 and 45 minutes after stress. All patients had coronary angiography correlation (15). In 44% of patients perfusion defects were significantly larger at 15 minutes compared to 45 minutes after stress. Images obtained at 15 minutes post stress correlated better with coronary angiography than the images at 45 minutes post stress. Early post stress imaging has been usually performed with ^{99m}Tc-tetrofosmin rather than ^{99m}Tc-sestamibi due to lower hepatic activity and a stable heart-to-liver ratio during the first 15 minutes after the injection of tetrofosmin (17, 18). The present study also demonstrates significantly larger perfusion defects on DR D-SPECT imaging in 55% of patients imaged 15-47 minutes post stress injection compared to 47-100 minutes post stress imaging by conventional SPECT. These differences were not demonstrated on the rest ^{201}Tl images of the same patients, and were also not seen in patients who were imaged on D-SPECT following conventional SPECT apart from one patient (patient 19, Table 2 and 3). Previous studies with ^{99m}Tc-sestamibi stress/rest protocol comparing D-SPECT to conventional SPECT when D-SPECT was performed following the conventional acquisition (5, 19) did also not reveal such differences. Therefore, although early post stress D-SPECT imaging was technically suboptimal in three of 24 patients (12.5%) our study shows it may have a role to improve the diagnostic accuracy of MPI. This needs to be further demonstrated in larger patient studies with angiographic correlation. Berman et al. (9) have recently described the use of a rapid D-SPECT stress ^{201}Tl/rest ^{99m}Tc labeled tracer myocardial perfusion imaging (sequential

dual-isotope imaging), beginning rest imaging within 2 minutes after rest injection. Good to excellent image quality was achieved in 96% of patients and, furthermore, this protocol demonstrated less extracardiac activity compared to standard rest imaging with a ^{99m}Tc/^{99m}Tc protocol. The rest images were acquired for 4 minutes within 2 minutes after rest injection, unlike the current study, where we acquired the data for 15 minutes at 75 minutes after stress injection on average and 35 minutes post stress injection in patients imaged “early”, when variable liver and gut activity may interfere with the scan quality.

Early post-stress imaging may cause artifacts. Friedman et al. (20) have described an upward movement (“upward creep”) of the heart of 2 pixels or more during early post stress acquisition of ^{201}Tl (5-15 minutes after treadmill exercise) causing artifactual reversible ^{201}Tl defects localized in the inferior and basal inferoseptal walls. In our study, however, we employed pharmacologic exercise with adenosine, early post stress DR D-SPECT acquisitions were performed at the earliest 15 minutes post stress injection and stress and rest data were acquired simultaneously. Therefore it would be expected that any artifacts will have similar effects on both data sets. In addition, in our study the discrepancies between DR D-SPECT and conventional SPECT involved mainly the antero-apical region and septum and the inferior wall was involved only in one case. In this case the entire septum, not only the infero-septal region showed also a more prominent perfusion defect on the DR D-SPECT compared to conventional SPECT.

Fewer discrepancies were noted between the rest images of DR D-SPECT and conventional SPECT. This may be due to the better sensitivity and resolution of the D-SPECT and to the scatter corrected images. Since the DR acquisition followed conventional SPECT rest acquisition there could also be redistribution of ^{201}Tl between these two acquisitions. However, Backus et al. (21) have recently demonstrated in 102 patients who were injected with ^{201}Tl at rest and imaged at rest and again after stress there were no significant differences in tracer activity in normal and ischemic regions between these two acquisitions.

Study limitations

This study is a feasibility study, and we have demonstrated the ability to perform simultaneous DR imaging on a solid state camera. The imaging protocol enabled comparison to conventional SPECT. Following these initial results further developments of protocols such as a simultaneous acquisition of rest ^{99m}Tc-MIBI/stress ^{201}Tl will allow taking advantage of the high first-pass extraction fraction of ^{201}Tl at high flow rates compared with the ^{99m}Tc-labelled tracers (11). With the improved sensitivity of D-SPECT the relative injected doses and the time of acquisition can also be modified in future studies, to reduce radiation exposure and spillover.

In this study ^{201}Tl was injected at rest, but the simultaneous DR images were acquired after stress. Since a separate D-SPECT rest acquisition was not performed it may be speculated there are changes in ^{201}Tl distribution following stress. However, Backus et al. have recently studied 102 patients who were injected with ^{201}Tl at rest, imaged at rest, then performed exercise without additional tracer injection and imaged again. There were no significant differences between the washout from normal and ischemic myocardium between these two imaging sessions (21). Therefore the imaging protocol used in our study is valid.

Another limitation in our comparison was that the DR D-SPECT studies were not only corrected for spillover but were also scatter corrected. Scatter correction was not part of the normal clinical protocol with conventional SPECT and was therefore not applied.

CONCLUSION

The present study demonstrates the feasibility of a single 15 minute list mode simultaneous dual-radionuclide acquisition with D-SPECT employing spillover and scatter correction reconstruction. The results of the present study demonstrate comparable diagnostic performance and image quality of DR D-SPECT and conventional SPECT. Furthermore, early post-stress DR D-SPECT showed significantly larger perfusion defects compared to conventional SPECT in 45% of patients. If proven in larger patient studies this may potentially improve the diagnostic accuracy of myocardial perfusion imaging. Modifications of the injected doses and of the imaging protocol with DR D-SPECT may enable shortening of imaging time, reducing radiation exposure and shortening significantly patient stay in the department.

Acknowledgments

This work was undertaken at UCLH/UCL who received a proportion of funding from the department of Health's NIHR Biomedical Research Centres funding scheme

REFERENCES

1. Patton JA, Slomka P, Germano G, Berman D. Recent technological advances in nuclear cardiology. J Nucl Cardiol. 2007; 14:501–513. [PubMed: 17679058]
2. Slomka PJ, Patton JA, Berman DS, Germano G. Advances in technical aspects of myocardial perfusion SPECT imaging. J Nucl Cardiol. 2009; 16:255–276. [PubMed: 19242769]
3. Gambhir SS, Berman DS, Ziffer J, Nagler M, Sandler M, Patton J, Hutton B, Sharir T, Ben-Haim S, Ben-Haim S. A novel high-sensitivity rapid-acquisition single-photon cardiac imaging camera. J Nucl Med. 2009; 50:635–643. [PubMed: 19339672]
4. Erlandsson K, Kacperski K, Van Gramberg D, Hutton BF. Performance evaluation of D-SPECT: a novel SPECT system for nuclear cardiology. Phys Med Biol. 2009; 54:2635–2649. [PubMed: 19351981]
5. Sharir T, Ben-Haim S, Merzon K, Prochorov V, Dickman D, Ben-Haim S, Berman DS. High-speed myocardial perfusion imaging: Initial clinical comparison with conventional dual detector Anger camera imaging. J Am Coll Cardiol Img. 2008; 1:156–163.
6. Kacperski, K.; Erlandsson, K.; ben-Haim, S.; Van Gramberg, D.; Hutton, BF. Iterative deconvolution of simultaneous dual radionuclide projections for CdZnTe based cardia SPECT; Proc IEEE Nucl Sci Symp Med Imaging Conf; 2008; p. 5260-5263.Abstr
7. Hudson HM, Larkin RS. Accelerated image reconstruction using ordered subsets of projection data. IEEE Trans Med Imaging. 1994; 13:601–609. [PubMed: 18218538]
8. Berman DS, Kiat H, Friedman JD, et al. Separate acquisition rest thallium-201/stress technetium-99m seatamibi dual-isotope myocardial perfusion single-photon emission computed tomography: a clinical validation study. J Am Coll Cardiol. 1993; 22:1455–1464. [PubMed: 8227805]
9. Berman DS, Kang X, Tamarappoo B, Wolak A, Hayes SW, Nakazato R, Thomson LEJ, Kite F, Cohen I, Slomka PJ, Einstein AJ, Friedman JD. Stress thallium-201/rest technetium −99m sequential dual isotope high-speed myocardial perfusion imaging. J Am Coll Cardiol Img. 2009; 2:273–282.
10. Ben-Haim S, Hutton BF, Van Gramberg D, et al. Simultaneous dual isotope myocardial perfusion imaging (DI MPI) with D-SPECT (abstr). J Nucl Cardiol. 2008; 15:52.
11. Kiat H, Germano G, Friedman J, Van Train K, Silagan G, Wang FP, Maddahi J, Berman D. Comparative feasibility of separate or simultaneous rest Thallium201/stress Technetioum-99m-sestamibi dual-isotope myocardial perfusion SPECT. J Nucl Med. 1994; 35:542–548. [PubMed: 8151372]
12. Ito Y, Uehara T, Fukuchi K, Tsujimura E, Hasegawa S, Nishimura T. Comparison of dual-isotope acquisition of ^{201}Tl and ^{99}Tc^{m}-tetrofosmin for the detection of ischaemic heart disease and

determination of the optimal imaging time of $^{99}Tc^{m}$-tetrofosmin. Nucl Med Commun. 1998; 19:119–126. [PubMed: 9548195]

13. Weinmann P, Faraggi M, Moretti JL, Hannequin P. Clinical validation of simultaneous dual-isotope myocardial scintigraphy. Eur J Nucl Med Mol Imaging. 2003; 30:25–31. [PubMed: 12483406]
14. Steele PP, Kirch DL, Koss JE. Comparison of simultaneous dual-isotope multipinhole SPECT with rotational SPECT in a group of patients with coronary artery disease. J Nucl Med. 2008; 49:1080–1089. [PubMed: 18552149]
15. Giorgetti A, Rossi M, Stanislao M, Valle G, Bertolaccini P, Maneschi A, Giubinni R, De Rimini ML, Mazzanti M, Cappagli M, Milan E, Volterrani D, Marzullo P, the Myoview Imaging group. Feasibility and diagnostic accuracy of a gated-SPECT early imaging protocol: A multicenter study of the Myoview Imaging Optimization group. J Nucl Med. 2007; 48:1670–1675. on behalf of. [PubMed: 17873126]
16. Schulz G, Oswald E, Kaiser HJ, wom Dahl J, Kleinhans E, Buell E. Cardiac stress-rest single-photon emission computed tomography with technetium 99m-labeled tetrofosmin: influence of washout kinetics on regional myocardial uptake values of the rest study with a 1-day protocol. J Nucl Cardiol. 1997; 4:298–301. [PubMed: 9278876]
17. Sinusas AJ, Shi Q-X, SAltzberg MT, et al. Technetium-99m-tetrofosmin to assess myocardial blood flow: Experimental validation in an intact canine model of ischemia. J Nucl Med. 1994; 35:664–671. [PubMed: 8151391]
18. Flamen P, Bossuyt A, Franken PR. Technetium-99m-tetrofosmin in dipyridamole-stress myocardial SPECT imaging: Intraindividual comparison with technetium-99m-sestamibi. J Nucl Med. 1995; 36:2009–2015. [PubMed: 7472590]
19. Ben-Haim S, Sharir T, Hutton BF, Van Gramberg D, Prvulovich EM, Bomanji JB, Groves AM, Waddington WA, Dickman D, Ell PJ. Quantitative analysis of fast myocardial perfusion imaging with D-SPECT: Comparison to conventional SPECT (abstr). Eur J Nucl Med Mol Imaging. 2008; 35(suppl 2):S160.
20. Friedman J, Van Train K, Maddahi J, Rozanski A, Prigent F, Bietendorf J, Waxman A, Berman DS. “Upward creep” of the heart: A frequent source of false-positive reversible defects during Thallium-201 stress-redistribution SPECT. J Nucl Med. 1989; 30:1718–1722. [PubMed: 2795212]
21. Backus BE, Verburg FA, Konijnenberg MW, Verzijlbergen JF. Myocardial perfusion SPECT: rest and stress in one acquisition (abstr.). J Nucl Cardiol. 2008; 15:S19.

Europe PMC Funders Author Manuscripts

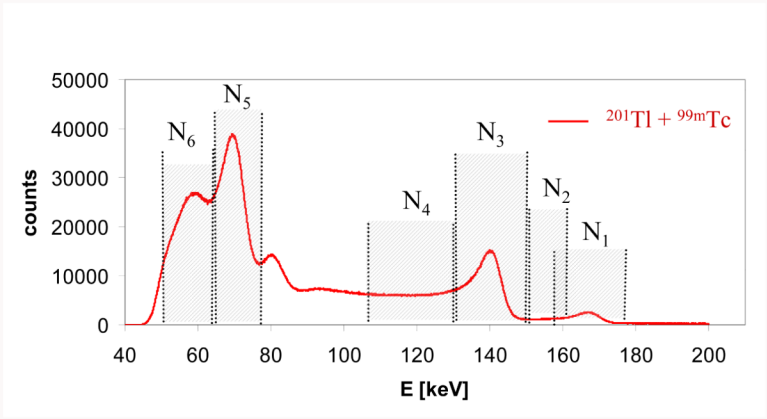

Figure 1.

A combined energy spectrum for ^{99m}Tc and ^{201}Tl is plotted together with the energy windows selected for the dual radionuclide acquisition (N1-N6). These correspond to photopeaks for the two radionuclides (N1, N3, N5) and energy windows that estimate scatter and cross-talk (N2, N4, N6). Note that the algorithm can accommodate overlapping windows (e.g. N1, N2).

Europe PMC Funders Author Manuscripts

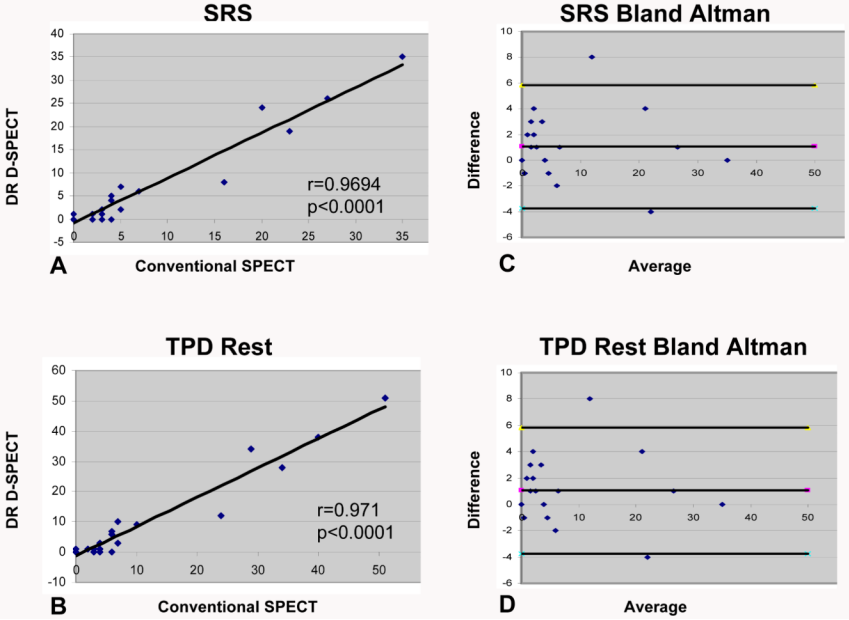

Figure 2.

Correlation between DR D-SPECT and conventional SPECT for (**A**) summed rest score (r=0.9657, p<0.0001) and (**B**) % total perfusion defect at rest (r=0.9665, p<0.0001). Bland-Altman graphs showing good agreement between SRS (**C**) and % total perfusion defect (**D**) of DR D-SPECT and conventional SPECT with a mean difference of 0.79, 95% confidence interval −2.459-0.428 for SRS; mean difference 1.16, 95% confidence interval −3.54-0.627 for %TPD rest.

DR=dual radionuclide; SRS= summed rest score; %TPD= % total perfusion defect.

Europe PMC Funders Author Manuscripts

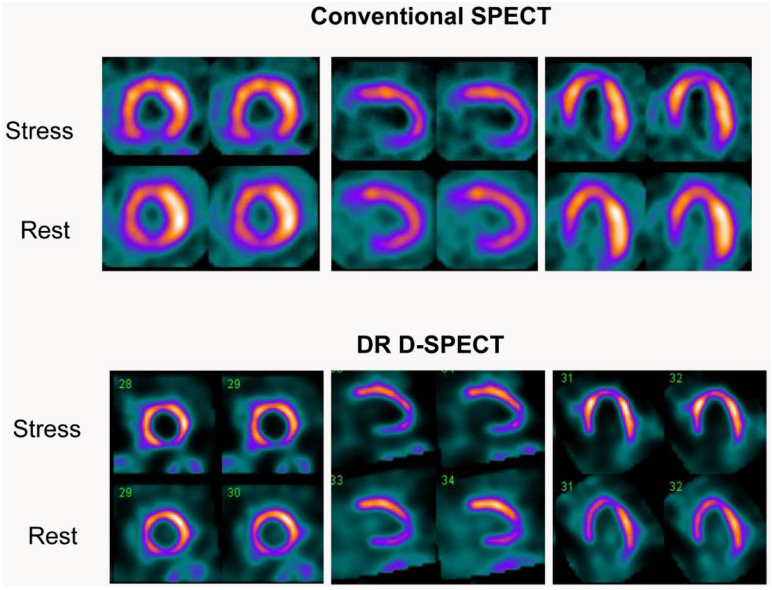

Figure 3.
66 year old male with atypical angina and shortness of breath. Known occluded RCA. Conventional SPECT images (top) showed absent uptake in the basal inferior wall and a stress induced infero-apical defect. Rest images showed infero-apical improvement. DR D-SPECT (bottom) showed similar findings.
RCA = right coronary artery; DR = dual radionuclide

Europe PMC Funders Author Manuscripts

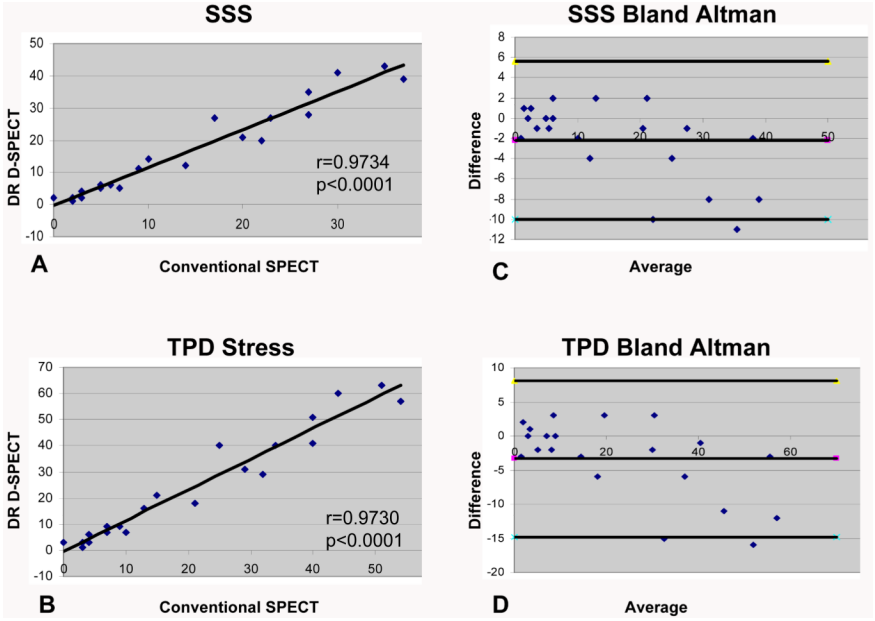

Figure 4.

Correlation between DR D-SPECT and conventional SPECT for (**A**) summed stress score (r=0.9790, p<0.0001) and (**B**) % total perfusion defect at stress (r=0.9784, p<0.0001). Bland-Altman graphs showing good agreement between SSS (**C**) and % total perfusion defect (**D**) of DR D-SPECT and conventional SPECT with a mean difference of −2.0, 95% confidence interval −2.392-1.991 for SSS; mean difference −3.0, 95% confidence interval −3.42-3.076 for % TPD stress.

DR=dual radionuclide; SSS= summed stress score; %TPD= % total perfusion defect.

Europe PMC Funders Author Manuscripts

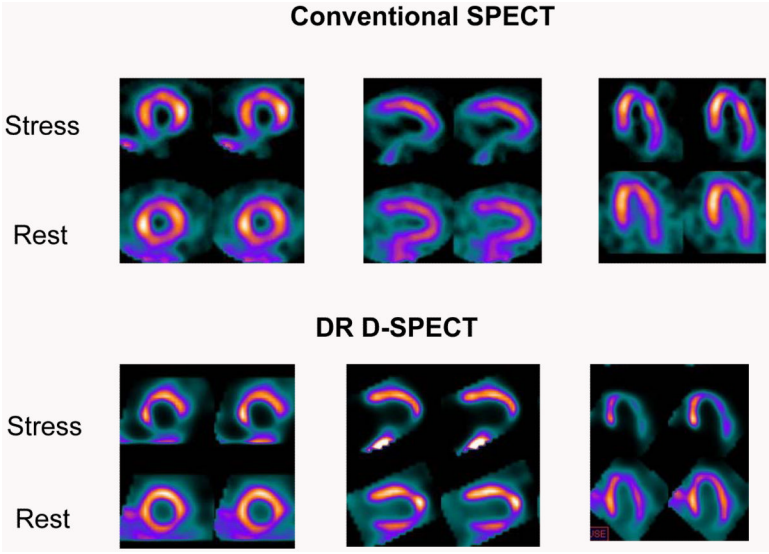

Figure 5.
39 year old male with previous history of inferior wall infarction, RCA and LAD PCI. In addition there is a known LCX lesion. Conventional SPECT (top) showed a stress induced inferior and apical perfusion defect with a possible stress induced defect in the septum, while DR D-SPECT showed the same abnormalities but more prominently and added a stress induced perfusion defect in the inferolateral wall. Coronary angiography 80 days after MPI showed 70% LAD in-stent restenosis, short focal 80% LCX stenosis and proximal occlusion of RCA. The patient was referred for CABG.
RCA= right coronary artery; LAD=left anterior descending artery; PCI= percutaneous intervention; LCX= left circumflex artery; DR = dual-radionuclide; MPI= myocardial perfusion imaging; CABG = coronary artery bypass graft surgery.

Europe PMC Funders Author Manuscripts

Europe PMC Funders Author Manuscripts

TABLE 1

Clinical characteristics

Characteristics	N=25
Age (yrs)	64.5 ±11.8
Male (%)	16 (64)
BMI	25.6 ± 2.64
Diabetes Mellitus (%)	9 (36)
Hypertension (%)	15 (60)
Hypercholesterolemia (%)	14 (56)
History of CAD (%) MI (%) PCI (%) CABG (%)	21 (84) 7 (28) 12 (48) 5 (20)

BMI = Body mass index; CAD = coronary artery disease; MI = Myocardial infarction; PCI = Percutaneous coronary intervention; CABG = coronary artery bypass graft surgery.

Europe PMC Funders Author Manuscripts

Table 2

Patients with ≥ 5% differences in total perfusion defect at stress between DR D-SPECT and conventional SPECT

		DR D-SPECT		SPECT		
Pt	**Gender**	**Acquisition time p/stress (min)**	**TPD-S (%)**	**Acquisition time p/stress (min)**	**TPD-S (%)**	**Myocardial region with larger TPD-S difference**
19	F	124	60	75	44	Antero-apical
20	M	47	21	100	15	Antero-apical
21	M	18	63	60	51	Inferior and septum
22	F	20	40	47	34	Antero-septal, apex
23	F	18	51	62	40	Apex, septum, anterior, lateral
25	M	18	40	45	25	Apex, septum, lateral

DR= simultaneous dual radionuclide; SPECT=conventional SPECT; Pt=patient; TPD-S=Total perfusion defect at stress

Europe PMC Funders Author Manuscripts

Table 3

Patients with ≥ 5% differences in total perfusion defect at rest between DR D-SPECT and conventional SPECT

		DR D-SPECT		SPECT		
Pt	**Gender**	**Acquisition time p/rest injection (min)**	**TPD-R (%)**	**Acquisition time p/rest injection (min)**	**TPD-R (%)**	**Myocardial region with TPD-R difference**
11	F	185	28	30	34	Apical lateral
17	F	150	12	55	24	Anteroseptal
19	F	231	34	39	29	Anteroapical

DR= simultaneous dual radionuclide; SPECT=conventional SPECT; Pt=patient; TPD-R=total perfusion defect at rest

Eur J Nucl Med Mol Imaging. Author manuscript; available in PMC 2011 June 06.

Europe PMC Funders Author Manuscripts

Table 4

Results of myocardial perfusion studies in patients with coronary angiography

Simultaneous DR DSPECT						Conventional SPECT			
Pt	**Gender**	**TPD-S (%)**	**TPD-R (%)**	**Isch**	**MI**	**TPD-S (%)**	**TPD-R (%)**	**Isch**	**MI**
3	M	18	10	Inf-ap; Inf-lat	Inf	21	7	Inf-ap; Inf-lat	Inf
4	M	31	7	Inf-lat	Inf	29	6	Inf-lat	Inf
18	M	7	1	Inf; Mid-ant	No	10	4	Inf; Mid-ant	No
*19	F	63	35	Inf-lat Ant-ap	Inf-lat	54	29	Inf-lat Ant-ap	Inf-lat
*25	M	40	6	Inf, Lat, Sept, Ap	No	25	6	Inf	No

DR = dual radionuclide; Pt = Patient; TPD-S = Total perfusion defect at stress; TPD-R = Total perfusion defect at rest; Isch = Ischemia; MI = Myocardial infarction; Inf-ap = Infero-apical; Inf-lat = infero-lateral; Inf = Inferior; Mid-ant = Mid-anterior; Ant-ap = antero-apical; Lat = lateral; Sept = septum; Ap = apical

* - Patients 19 and 25 had significantly more ischemia on simultaneous DR D-SPECT compared to conventional SPECT. (see also Table 2)

Europe PMC Funders Author Manuscripts

Table 5

Coronary angiography results

Patient Number	Angiographic result	Procedure
3	LCX: tight stenosis	PCI of LCX
4	RCA: stenosis before crux and 2 stenoses in the PDA.	PCI of RCA and PDA
18	D1: Moderate ostial stenosis; OM1: moderate stenosis	None
19	D1: 60% mid vessel stenosis OM1: 70% stenosis RCA: Mid vessel occlusion	PCI of RCA
25	LAD: 70% distal in-stent stenosis; LCX: short 80% stenosis; RCA: proximal occlusion.	CABG

LCX = left circumflex; PCI = percutaneous intervention; RCA = right coronary artery; PDA = posterior descending artery; D1 = first diagonal branch; OM1 = first obtuse marginal branch; LAD = left anterior descending; CABG = coronary artery bypass graft surgery.